Dimensionality Reduction in Control and Coordination of the Human Hand

Ramana Vinjamuri, *Member, IEEE*, Mingui Sun, *Senior Member, IEEE*, Cheng-Chun Chang, *Member, IEEE*, Heung-No Lee, *Member, IEEE*, Robert J. Sclabassi, *Senior Member, IEEE*, and Zhi-Hong Mao*, *Senior Member, IEEE*

***Abstract*—The concept of kinematic synergies is proposed to address the dimensionality reduction problem in control and coordination of the human hand. This paper develops a method for extracting kinematic synergies from joint-angular-velocity profiles of hand movements. Decomposition of a limited set of synergies from numerous movements is a complex optimization problem. This paper splits the decomposition process into two stages. The first stage is to extract synergies from rapid movement tasks using singular value decomposition (SVD). A bank of template functions is then created from shifted versions of the extracted synergies. The second stage is to find weights and onset times of the synergies based on l_1-minimization, whose solutions provide sparse representations of hand movements using synergies.**

***Index Terms*—Grasping, human hand, kinematic synergies, l_1-minimization, rehabilitation, virtual reality.**

I. Introduction

THE HUMAN hand has a large number of mechanical DOF, which offers tremendous flexibility to perform skilled finger movements. Such flexibility makes the control of the hand very challenging. Nevertheless, the central nervous system (CNS) seems to handle the complexity and high dimensionality in movement control with amazing ease and absence of effort. Researchers have been confronted by the high DOF control problems when attempting to understand physiology behind the movements and to mimic the CNS in various applications like brain–computer interface (BCI), robotics, telesurgery, and neuroprosthesis. These problems have been addressed by different theories on dimensionality reduction, many of which converge at an endeavor of extracting synergies, to list a few relevant [1]–[7].

Synergies are hypothesized to address the key problems that are posed to the CNS in control and coordination of available DOF. Though named the same, synergies have different meanings. In many contexts, synergies are common (shared) spatiotemporal patterns in muscle activities or movement kinematics/dynamics. These patterns can be used as primitives or building blocks, which can be combined to form complete movements. In this paper, kinematic synergies observed in angular velocity profiles of joint movements of the hand will be referred to as hand synergies. Our definition of synergies is inspired by d'Avella *et al.* [5] and can be interpreted by a convolutive-mixture model for movement generation [8]. According to this model (see Section II-A), commands in the form of impulse trains originated in the CNS convolve with the pattern generators in the lower level neural and biomechanical systems to result in the generation of hand movements. Synergies can be viewed as impulse responses of these pattern generators.

The objective of this paper is to identify the hand synergies through developing an effective algorithm to decompose the joint-angular velocity profiles of the hand. Decomposition of a limited set of synergies from numerous movements is a complex optimization problem. One of our previous attempts [9] was to use an iterative gradient-descent method to decompose hand synergies following the approach of d'Avella *et al.* [5]. This method simultaneously searches for the waveforms of synergies and the parameters (weights and time shifts) characterizing the recruitments of synergies in movements. However, it may converge to local minima because of the nonconvex nature of the optimization problem. Moreover, this method requires long processing times, which make it inapplicable to time-critical implementations such as BCI.

In order to reduce the computational load, we split the decomposition process into two stages in this paper. The first stage is to extract the waveforms of synergies from rapid movement tasks using singular value decomposition (SVD) (details given in Section II-C). A bank of template functions is then created from shifted versions of the extracted synergies. The second stage is to find the weights and onset times of the synergies. The optimization problem in this stage can be formulated as an l_1-minimization problem, which can be efficiently solved by an interior-point method. The solutions to the l_1-minimization problem tend to select a sparse set of synergies or shifted versions of synergies from the bank of template functions constructed in the first stage. Compared with earlier methods [5], [9], the previous two-stage method greatly simplifies the computation and favors time-critical applications. Furthermore, this method accounts for multiple recruitments of a single synergy in a movement. Such reusability of a single synergy was not considered in other models, to our best knowledge.

Manuscript received April 12, 2009; revised July 29, 2009. First published September 29, 2009; current version published January 20, 2010. This work was supported by the National Science Foundation under Grant CMMI-0727256. *Asterisk indicates corresponding author.*

R. Vinjamuri is with the Department of Physical Medicine and Rehabilitation, University of Pittsburgh, Pittsburgh, PA 15213 USA (e-mail: rkv3@pitt.edu).

M. Sun and R. J. Sclabassi are with the Department of Neurological Surgery, University of Pittsburgh, Pittsburgh, PA 15213 USA, and also with the Computational Diagnostics, Inc., Pittsburgh, PA 15213 USA.

C.-C. Chang is with the Department of Electrical Engineering, National Taipei University of Technology, Taipei 106, Taiwan.

H.-N. Lee is with the Department of Information and Communications, Gwangju Institute of Science and Technology, Gwangju 500-712, Korea.

*Z.-H. Mao is with the Department of Electrical and Computer Engineering and the Department of Bioengineering, University of Pittsburgh, Pittsburgh, PA 15261 USA (e-mail: maozh@engr.pitt.edu).

Color versions of one or more of the figures in this paper are available online at http://ieeexplore.ieee.org.

Digital Object Identifier 10.1109/TBME.2009.2032532

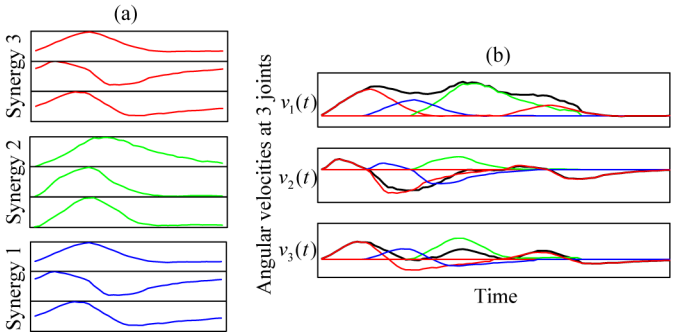

Fig. 1. Example of using three synergies (a) to construct joint-angular-velocity profiles at (b) three joints.

II. Methods

A. Model

An illustration of how synergies combine to form movement is shown in Fig. 1. In this figure, weighted combination of three time-varying synergies leads to the formation of a movement profile. This can be numerically represented as

$$\mathbf{v}(t) = \sum_{j=1}^{m} \sum_{k=1}^{K_j} c_{jk} \mathbf{s}^j (t - t_{jk}) \tag{1a}$$

or

$$v_i(t) = \sum_{j=1}^{m} \sum_{k=1}^{K_j} c_{jk} s_i^j (t - t_{jk}), \qquad i = 1, \ldots, n. \tag{1b}$$

In the previous equations, $\mathbf{v}(t)$ denotes $[v_1(t), \ldots, v_n(t)]'$, where $'$ represents transpose, $v_i(t)$ $(i = 1, \ldots, n)$ represents the angular velocity of the ith joint of the hand at time t, and n is the total number of the considered joints of the hand; a kinematic synergy is denoted $\mathbf{s}^j(t) \equiv [s_1^j(t), \ldots, s_n^j(t)]'$, where j ranges from 1 to m and m is the total number of synergies; K_j is the number of repeats of the jth synergy used in $\mathbf{v}(t)$, and c_{jk} and t_{jk} represent the amplitude coefficient and time shift, respectively, of the kth repeat of the synergy $\mathbf{s}^j(\cdot)$. Note that in Fig. 1, the first synergy is used twice (a shifted version of the first synergy is used at the end of the movement). Accommodating multiple recruitments of the same synergy can reduce the DOF or dimensionality in movement control and thus reduce computational load of the CNS.

The synergy-based movement generation can also be interpreted by a convolutive-mixture model proposed in [8]. The angular velocities of finger joints can be modeled as convolutive mixtures of some command signals represented by impulse trains (see Fig. 2). A command impulse (originated in the higher level neural system) evokes the activation of circuits in the neural system, then stimulates certain biomechanical structures, and eventually creates a stereotyped angular change at each finger-joint of the hand. This process can be viewed as the activation of a synergy [see Fig. 2(a)] and is similar to the production of impulse responses of a set of filters, each of which triggers the movement of a specific finger joint. The filters or synergy

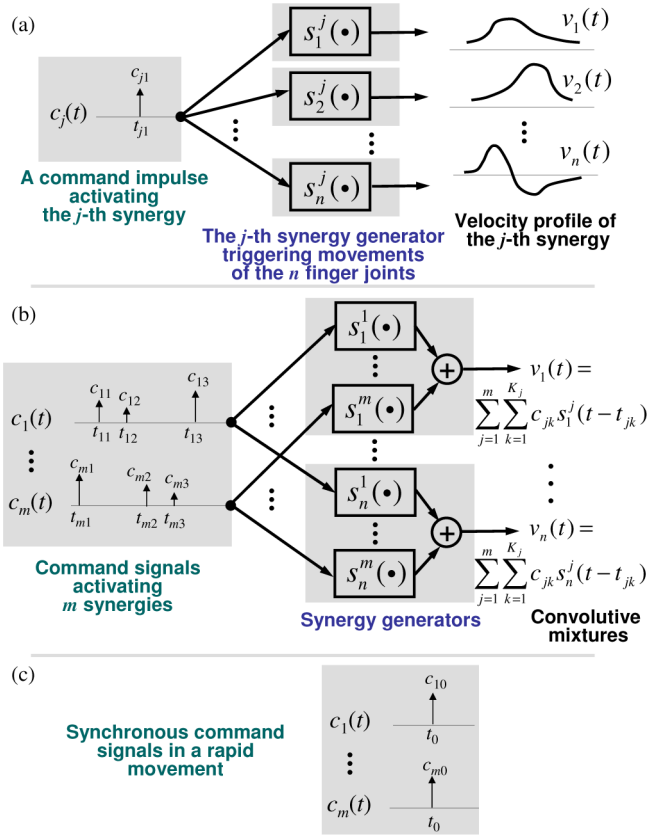

Fig. 2. Hypothesized model for generation of hand movement. (a) Kinematic synergy can be depicted as impulse responses of a set of filters. The filters summarize the related neural–biomechanical structures that trigger finger-joint movements in response to an impulse in the higher level neural system. (b) Movement profile of the hand can be modeled as convolutive mixtures of command impulses passing through the corresponding filters or synergy generators [8]. (c) Synchronous command signals (with the same onset time) in a rapid movement.

generators characterize the related neural–biomechanical structures that are responsible for the movement of finger joints in response to a command impulse. We assume that all the filters are linear and their impulse responses have finite durations. Thus, a movement profile of the hand can be modeled as the superposition of the impulse responses of the command impulses passing through the corresponding filters residing in the neural system and connected biomechanical system [see Fig. 2(b)]. A similar idea was already studied in [10], where Tresch *et al.* proposed that the CNS produces a range of movement through the combination of a small number of "unit burst generators" organized within the spinal cord. Mason *et al.* hypothesized that the eigenpostures or postural synergies may be represented in the discharge of a population of hand-related motor and premotor cortical cells [4].

Based on the earlier model, when the jth synergy generator is activated by an impulse with amplitude c_{j1} at time t_{j1} [see Fig. 2(a)], we obtain a hand movement with the following angular-velocity profile:

$$\mathbf{v}(t) = c_{j1} \mathbf{s}^j (t - t_{j1}).$$

When the jth synergy generator is activated by a command signal $c_j(t)$ containing a train of impulses with amplitudes c_{jk} at times t_{jk}, $k = 1, \ldots, K_j$, the angular-velocity profile of the finger joints becomes

$$\mathbf{v}(t) = (c_j * \mathbf{s}^j)(t) = \sum_{k=1}^{K_j} c_{jk}\mathbf{s}^j(t - t_{jk})$$

where $*$ represents convolution. When more than one synergies are considered [see Fig. 2(b)], the convolutive-mixture model can then be expressed by (1a) or (1b).

In the following, we will also consider a special type of movements, i.e., rapid hand movements. The human subjects performed these rapid movements to mimic the process of reacting to instantaneous impulses descending from the CNS. These rapid movements minimize the reaction times and constrain the synergies to combine instantaneously [see Fig. 2(c)]. Thus as a special case of the current model, the angular-velocity profile of a rapid movement can be achieved as a weighted summation of *synchronous* synergies as expressed in the following equation:

$$\mathbf{v}(t) = \sum_{j=1}^{m} c_{j0}\mathbf{s}^j(t - t_0) \tag{2}$$

where the impulses of $c_j(t)$, $j = 1, \ldots, m$, occur at the same time t_0 but may have different amplitude c_{j0}.

For different grasping tasks as described later in Section II-B, we use superscript g ($g = 1, 2, \ldots$) in $\mathbf{v}^g(t)$ to distinguish angular-velocity profiles of different movement tasks. If we shift all $\mathbf{v}^g(t)$ in time such that the movement onset times coincide with $t = 0$, then the time of impulses, t_0, in $\mathbf{v}^g(t)$ should be the same for all g, but the amplitudes of impulses, denoted c^g_{j0}, may be different for different g. Therefore, for task g, (2) can be rewritten as

$$\mathbf{v}^g(t) = \sum_{j=1}^{m} c^g_{j0}\mathbf{s}^j(t - t_0) \tag{3a}$$

or

$$v^g_i(t) = \sum_{j=1}^{m} c^g_{j0}s^j_i(t - t_0), \qquad i = 1, \ldots, n. \tag{3b}$$

Then we can use SVD to extract the synchronous synergies. Since $\mathbf{s}^j(t - t_0)$ has exactly the same waveform of $\mathbf{s}^j(t)$, it is equivalent to use $\mathbf{s}^j(t - t_0)$ ($j = 1, \ldots, m$) as the synergies. From now on, we simply write $\mathbf{s}^j(t - t_0)$ as $\mathbf{s}^j(t)$, ignoring the t_0 term.

B. Experiments

The experimental setup consisted of a right-handed CyberGlove [11] equipped with 22 sensors that can measure angles at all the finger joints. For the purpose of reducing computational burden, in this study, we only considered ten of the sensors that correspond to the metacarpophalangeal (MCP) and interphalangeal (IP) joints of the thumb and the MCP and proximal interphalangeal (PIP) joints of the other four fingers. These ten joints can capture most characteristics of the hand in grasping tasks. Note that the distal interphalangeal (DIP) joints were not considered because the motions of the DIP and PIP joints are highly dependent—it was observed that during natural movements the flexion of the DIP joint of a finger is about two-thirds of that of the PIP joint [12].

Ten right-hand-dominant subjects were tested in a set of behavioral tasks. The question of whether the handedness influences identification of synergies is not addressed in this paper. The existence of postural synergies has already been shown irrespective of the handedness [13]. The influence of handedness on kinematic synergies, though an interesting research question, is beyond the scope of this paper.

A typical task consisted of grasping the objects of various shapes and sizes. Objects (wooden and plastic) of different shapes (spheres, circular discs, rectangles, pentagons, nuts, and bolts) and different dimensions were used in the grasping tasks and were selected based on two strategies. One was gradually increasing sizes of similar shaped objects, and the other was using different shapes. Start and stop times of each task were signaled by computer-generated beeps. In each task, the subject was in a seated position, resting his/her right hand at a corner of a table and upon hearing the beep, grasped the object placed on the table. At the time of the start beep hand was in rest posture, and then the subject grasped the object and held it until the stop beep. Between the grasps, there was enough time for the subjects to avoid the affects due to fatigue on succeeding tasks. The experiment was split into two phases, training phase and testing phase, the difference in these two being the velocity of grasps and types of grasps.

In the training phase, subjects were instructed to rapidly grasp 50 objects, one at a time, to mimic the process of reacting to instantaneous impulses descending from the CNS. This was repeated for the same 50 objects, and thus, the whole training phase obtained 100 rapid grasps. Only these 100 rapid grasps were used in extracting synergies.

In the testing phase, subjects were instructed to grasp the previous 50 objects naturally (slower than the rapid grasp), and then repeat the same again. So far, the tasks involved only grasping action. To widen the scope of applicability of the synergies, subjects were also asked to pose 36 American Sign Language (ASL) postures. Here subjects would start from an initial posture and stop at one ASL posture. These postures consisted of ten numbers (0−9) and 26 alphabets (A–Z), as shown in [14]. Note that these movements are different from grasping tasks. This is the testing phase which consists of 100 natural grasps and 36 ASL postural movements. The synergies derived in the training phase were then used in the reconstruction of all movements in the testing phase.

C. Analysis

Compared with the time-varying synergy model proposed in our previous work [9], the current model (1a) allows repetitive uses of synergies in a single movement. Although this brings us closer to physiological reality, computationally the decomposition of synergies becomes more difficult. We need to determine not only the shapes of the synergies but also their onset times, amplitudes, and number of recruitments in the movement.

Instead of iteratively adjusting both the shaping and timing of the synergies simultaneously, we propose to take two steps: the first step is to determine the morphology of synergies, and the second step is to use the obtained synergies as templates to decompose the hand movements.

Step 1 (Extraction of Synchronous Synergies Via SVD): After obtaining the joint angles at various times from the rapid grasps, angular velocities were calculated. These angular velocities were filtered from noise. Only the relevant projectile movement (about 0.45 s or 39 samples at a sampling rate of 86 Hz) of the entire angular-velocity profile was preserved and the rest was truncated.

Next an angular-velocity matrix, denoted V, was constructed for each subject. Angular-velocity profiles of the ten joints corresponding to one rapid grasp were cascaded such that each row of the angular-velocity matrix represented one movement in time. The matrix consisted of 100 rows and $39 \times 10 = 390$ columns:

$$V = \begin{bmatrix} v_1^1(1) & \cdots & v_1^1(39) & \cdots & v_{10}^1(1) & \cdots & v_{10}^1(39) \\ \vdots & \vdots & \vdots & \vdots & \vdots & \vdots & \vdots \\ v_1^g(1) & \cdots & v_1^g(39) & \cdots & v_{10}^g(1) & \cdots & v_{10}^g(39) \\ \vdots & \vdots & \vdots & \vdots & \vdots & \vdots & \vdots \\ v_1^{100}(1) & \cdots & v_1^{100}(39) & \cdots & v_{10}^{100}(1) & \cdots & v_{10}^{100}(39) \end{bmatrix} \tag{4}$$

where $v_i^g(t)$ represents the angular velocity of joint i ($i = 1, \ldots, 10$) at time t ($t = 1, \ldots, 39$) in the gth rapid-grasping task ($g = 1, \ldots, 100$).

Then, SVD [15] was performed on the angular-velocity matrix V of each subject

$$V = U \Sigma S \tag{5}$$

where U is a 100-by-100 matrix, which has orthonormal columns so that $U'U = I_{100\times 100}$ (100-by-100 identity matrix); S is a 100-by-390 matrix, which has orthonormal rows so that $SS' = I_{100\times 100}$; and Σ is a 100-by-100 diagonal matrix: $\mathrm{diag}\{\lambda_1, \lambda_2, \ldots, \lambda_{100}\}$ with $\lambda_1 \geq \lambda_2 \geq \cdots \geq \lambda_{100} \geq 0$. Matrix V can be approximated by another matrix $\tilde{V}$ with reduced rank m by replacing Σ with Σ_m, which contains only the m largest singular values, i.e., λ_1, ..., λ_m (the other singular values are replaced by zeros). The approximation matrix $\tilde{V}$ can be written in a more compact form

$$\tilde{V} = U_m \, \mathrm{diag}\{\lambda_1, \ldots, \lambda_m\} \, S_m \tag{6}$$

where U_m is a 100-by-m matrix containing the first m columns of U and S_m is a m-by-390 matrix containing the first m rows of S. Denoting $W = U_m \, \mathrm{diag}\{\lambda_1, \ldots, \lambda_m\}$, we have

$$V \approx \tilde{V} = W S_m . \tag{7}$$

Then, each row of S_m is called a *principal component* (PC), and W is called the weight matrix.

For easy comparison, let us name the elements of S_m in a way similar to (4)

$$S_m \equiv \begin{bmatrix} s_1^1(1) & \cdots & s_1^1(39) & \cdots & s_{10}^1(1) & \cdots & s_{10}^1(39) \\ \vdots & \vdots & \vdots & \vdots & \vdots & \vdots & \vdots \\ s_1^m(1) & \cdots & s_1^m(39) & \cdots & s_{10}^m(1) & \cdots & s_{10}^m(39) \end{bmatrix} \tag{8}$$

and name the elements of W in the following way:

$$W = \begin{bmatrix} w_1^1 & \cdots & w_m^1 \\ \vdots & \vdots & \vdots \\ w_1^g & \cdots & w_m^g \\ \vdots & \vdots & \vdots \\ w_1^{100} & \cdots & w_m^{100} \end{bmatrix} . \tag{9}$$

According to (7), each row of V can be approximated by a linear combination of the m PCs, and according to (7), (4), (8), and (9), we have

$$v_i^g(t) \approx \sum_{j=1}^{m} w_j^g s_i^j(t) \tag{10}$$

for $i = 1, \ldots, 10$, $g = 1, \ldots, 100$, and $t = 1, \ldots, 39$.

Comparing (10) and (3b), we can see that (10) has been written in the form of (3b), and thus, the earlier SVD procedure has found a solution to the synergy-extraction problem: the angular-velocity profiles (obtained by rearranging all joints rowwise for the PCs)

$$\begin{bmatrix} s_1^j(1) & \cdots & s_1^j(39) \\ s_2^j(1) & \cdots & s_2^j(39) \\ \vdots & \vdots & \vdots \\ s_{10}^j(1) & \cdots & s_{10}^j(39) \end{bmatrix}, \qquad j = 1, \ldots, m$$

can be viewed as a set of candidates of the synergies. According to (7) or (10), these synergies can serve as "building blocks" to reconstruct joint-angular-velocity profiles of hand movements.

To decide m, the number of PCs or synergies that we want to use in reconstruction of the testing movements, we consider the accuracy of approximation in (7) or (10). The approximation accuracy can be measured by an index defined as

$$\frac{\lambda_1^2 + \lambda_2^2 + \cdots + \lambda_m^2}{\lambda_1^2 + \lambda_2^2 + \cdots + \lambda_{100}^2}.$$

The larger this index is, the closer the approximation is. This index also provides indication of the fraction of total variance of the data matrix accounted by the PCs. To ensure satisfactory approximation, the index should be greater than some threshold. In this study, we used 95% as the threshold (a commonly used threshold [15]) to determine the number of PCs or synergies (i.e., m).

Step 2 (Decomposition of Hand Movements Via l_1-Minimization): The second step is to use the synergies obtained from step 1) as templates to decompose the hand movements. In the following, we consider a matrix representation of the convolutive-mixture model. Such representation will ease the formulation of the movement decomposition problem as an l_1-minimization problem.

Let us assume for a subject m synergies were obtained. The duration of the synergies is t_s samples ($t_s = 39$ in this paper). Consider an angular-velocity profile of the subject, $\{\mathbf{v}(t), t = 1, \ldots, T\}$, where T ($T = 82$ in this paper) represents the movement duration (in samples). This profile can be rewritten as a row vector, denoted $\mathbf{v}_{\text{row}}$, as follows:

$$\mathbf{v}_{\text{row}} = [v_1(1), \ldots, v_1(T), \ldots, v_{10}(1), \ldots, v_{10}(T)].$$

Similarly, a synergy $\mathbf{s}^j(\cdot)$ can be rewritten as the following row vector:

$$[s_1^j(1), \ldots, s_1^j(t_s), 0, \ldots, 0, \ldots, s_{10}^j(1), \ldots, s_{10}^j(t_s), 0, \ldots, 0].$$

We add $T - t_s$ zeros after each $s_i^j(t_s)$ ($i = 1, \ldots, 10$) in the previous vector in order to make the length of the vector the same as that of $\mathbf{v}_{\text{row}}$. If the synergy is shifted in time by t_{jk} ($t_{jk} \leq T - t_s$) samples, then we obtain the following row vector:

$$[0, \ldots, 0, s_1^j(1), \ldots, s_1^j(t_s), 0, \ldots, 0, \ldots, 0, \ldots, 0, s_{10}^j(1), \ldots, s_{10}^j(t_s), 0, \ldots, 0]$$

with t_{jk} zeros added before each $s_i^j(1)$ and $T - t_s - t_{jk}$ zeros added after each $s_i^j(t_s)$.

Then, we construct a matrix as shown in (11) (at the bottom of this page) consisting of the row vectors of the synergies and all their possible shifts with $1 \leq t_{jk} \leq T - t_s$. Fig. 3 demonstrates the construction of such a matrix.

With the previous notation, the model (1a) or (1b) can be reexpressed as

$$\mathbf{v}_{\text{row}} = \mathbf{c}B \tag{12}$$

where $\mathbf{c}$ denotes

$$[0, \ldots, c_{11}, \ldots, 0, \ldots, c_{1K_1}, \ldots, 0, \ldots, c_{m1}, \ldots, 0, \ldots, c_{mK_m}, \ldots, 0]$$

with nonzero values c_{jk} appearing at the $(T - t_s + 1)(j - 1) + t_{jk}$th elements of $\mathbf{c}$. The matrix B can be viewed as a bank or library of template functions with each row of B as a template. This bank can be overcomplete and contain linearly dependent subsets. Therefore, for a given movement profile $\mathbf{v}_{\text{row}}$ and an overcomplete bank of template functions B, there exists an infinite number of $\mathbf{c}$ satisfying (12).

We hypothesize that the CNS' strategy for dimensionality reduction in movement control is to use a small number of synergies and a small number of recruitments of these synergies for movement generation. Therefore, the coefficient vector $\mathbf{c}$ in (12) should be sparse, i.e., having a lot of zeros and only a small number of nonzero elements. Therefore, we seek the sparsest coefficient vector $\mathbf{c}$ such that $\mathbf{c}B = \mathbf{v}_{\text{row}}$.

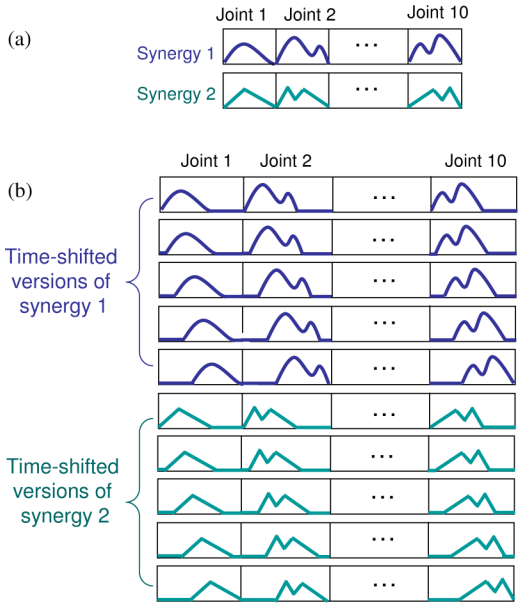

Fig. 3. Construction of the template matrix from synergies.

Formally, we aim to solve the optimization problem

$$\text{Minimize} \quad \| \mathbf{c} \|_0 \quad \text{subject to} \quad \mathbf{c}B = \mathbf{v}_{\text{row}} \tag{13}$$

where the l_0 norm $\| \mathbf{c} \|_0$ is the number of nonzeros in $\mathbf{c}$. In general, (13) is difficult to solve, because it requires enumerating subsets of the bank B to find the smallest subset able to represent $\mathbf{v}_{\text{row}}$ [16]. The complexity of such a subset search grows exponentially with number of elements in the bank [16].

Instead of solving (13) directly, we can consider an approximation of it using l_1-minimization

$$\text{Minimize} \quad \| \mathbf{c} \|_1 \quad \text{subject to} \quad \mathbf{c}B = \mathbf{v}_{\text{row}} \tag{14}$$

where the l_1 norm $\| \mathbf{c} \|_1$ is the sum of the absolute values of the elements of $\mathbf{c}$. The l_1-minimization problem (14) can be considered as a kind of convexification of (13): (14) is the closest convex optimization problem to (13) [16]. The added

$$B \equiv \begin{bmatrix} s_1^1(1) & \cdots & s_1^1(t_s) & 0 & \cdots & 0 & \cdots & s_{10}^1(1) & \cdots & s_{10}^1(t_s) & 0 & \cdots & 0 \\ 0 & s_1^1(1) & \cdots & s_1^1(t_s) & \cdots & 0 & \cdots & 0 & s_{10}^1(1) & \cdots & s_1^1(t_s) & \cdots & 0 \\ \vdots & \ddots & \ddots & \ddots & \ddots & \vdots & \cdots & \vdots & \ddots & \ddots & \ddots & \ddots & \vdots \\ 0 & \cdots & 0 & s_1^1(1) & \cdots & s_1^1(t_s) & \cdots & 0 & \cdots & 0 & s_{10}^1(1) & \cdots & s_{10}^1(t_s) \\ \vdots & \vdots & \vdots & \vdots & \vdots & \vdots & \vdots & \vdots & \vdots & \vdots & \vdots & \vdots & \vdots \\ s_1^m(1) & \cdots & s_1^m(t_s) & 0 & \cdots & 0 & \cdots & s_{10}^m(1) & \cdots & s_{10}^m(t_s) & 0 & \cdots & 0 \\ 0 & s_1^m(1) & \cdots & s_1^m(t_s) & \cdots & 0 & \cdots & 0 & s_{10}^m(1) & \cdots & s_1^m(t_s) & \cdots & 0 \\ \vdots & \ddots & \ddots & \ddots & \ddots & \vdots & \cdots & \vdots & \ddots & \ddots & \ddots & \ddots & \vdots \\ 0 & \cdots & 0 & s_1^m(1) & \cdots & s_1^m(t_s) & \cdots & 0 & \cdots & 0 & s_{10}^m(1) & \cdots & s_{10}^m(t_s) \end{bmatrix}. \tag{11}$$

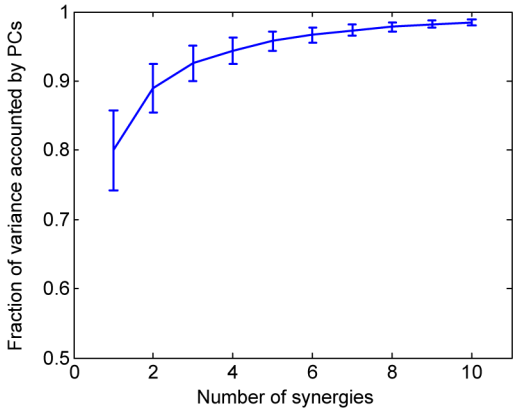

Fig. 4. Fraction of variance accounted by increasing number of PCs or synergies. Error bars indicate the standard deviation across subjects.

benefits of using l_1-minimization include that it can produce sparse solutions to $\mathbf{c}B = \mathbf{v}_{\text{row}}$ [17].

Note that in (12) we ignored the measurement noise and unmodeled nonlinearity. A more realistic form of (12) should be

$$\mathbf{v}_{\text{row}} = \mathbf{c}B + \mathbf{n} \tag{15}$$

where $\mathbf{n}$ is a residue due to noise or inaccuracy of the model. Because of this residue, we can no longer force $\mathbf{v}_{\text{row}} = \mathbf{c}B$ in (14). Therefore, we eliminate this constraint and add to the cost function a penalty term that prescribes a high cost to those values of $\mathbf{c}$ deviating from this constraint; we reformulate (14) into the following optimization problem:

$$\text{Minimize} \quad \| \mathbf{c} \|_1 + \frac{1}{\lambda} \| \mathbf{c}B - \mathbf{v}_{\text{row}} \|_2^2 \tag{16}$$

where $\| \cdot \|_2$ represents the l_2 norm or Euclidean norm of a vector and λ is a regulation parameter. In this study, we set $\lambda = 0.01\lambda_{\max}$, where $\lambda_{\max}$ denotes the l_∞ norm of $2\mathbf{v}_{\text{row}}B'$—see [18] for a detailed discussion on the determination of λ. Our choice of the regulation parameter has been able to achieve a reasonable balance between sparse solutions and good approximations to $\mathbf{v}_{\text{row}} = \mathbf{c}B$. This optimization problem, (16), can be efficiently solved by modern interior-point methods [18].

III. Results

A. Extraction of Synchronous Synergies

In the extraction of synchronous synergies (step 1), for all the ten subjects, on average the first PC or synergy accounted for approximately 80% of the total variance. The first and second PCs together accounted for about 89% of the total variance. In order to help determine how many PCs would suffice to account for the variance of the entire training data, a PC-variation chart is plotted in Fig. 4. Error bars indicate standard deviation across the ten subjects. For most of the subjects the first six PCs or synergies accounted for more than 95% of the total variance. Beyond six PCs there was not much appreciable contribution of higher order PCs in the total variance.

Angular-velocity profiles of six kinematic synergies obtained for subject 1 are depicted in Fig. 5. Across the rows are the ten

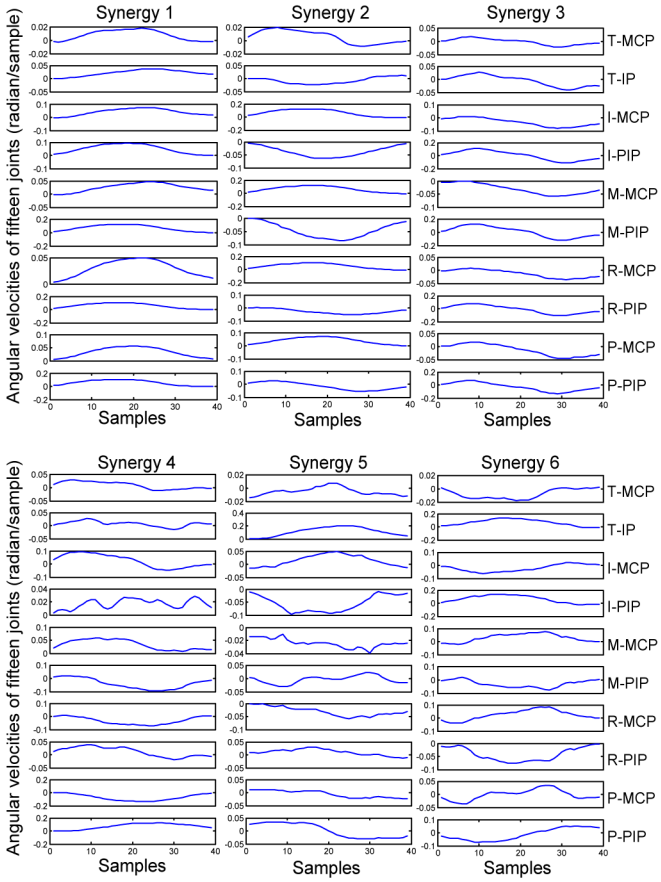

Fig. 5. Six kinematic synergies obtained for subject 1. Each synergy is about 0.45 s in duration (39 samples at 86 Hz). Abbreviations: T, thumb; I, index finger; M, middle finger; R, ring finger; P, pinky finger; MCP, metacarpophalangeal joint; IP, interphalangeal joint; PIP, proximal IP joint.

joints corresponding to the five fingers (two for each). These synergies show that peak velocities of the grasp occurred at the middle of the task. This reflects acceleration at the beginning of the task, which was generally open loop. It was followed by deceleration caused due to error feedback from sensory and motor systems while reaching the precise position of object, and finally closing of the grasp.

Given the initial posture, the temporal variation of postures along each kinematic synergy can be calculated via integration. Thus, temporal postural synergies were obtained from the earlier kinematic synergies. A set of six such temporal postural synergies obtained from subject 1 are depicted in Fig. 6(a). In the figure, four postures are snapshots at 25%, 50%, 75%, and 100% of the task times, respectively. End posture of each synergy indicates the contribution of synergy in a particular type of grasp. End postures of the six synergies for the remaining nine subjects are shown in Fig. 6(b). As all the subjects performed tasks on the same training objects, there were similarities in synergies adapted, among the subjects.

B. Reconstruction of Hand Movements Via l_1-Minimization

By linearly combining the extracted synergies, for each subject 100 natural (slower than rapid) grasping tasks and 36 ASL gesturing tasks which comprise the testing data, were

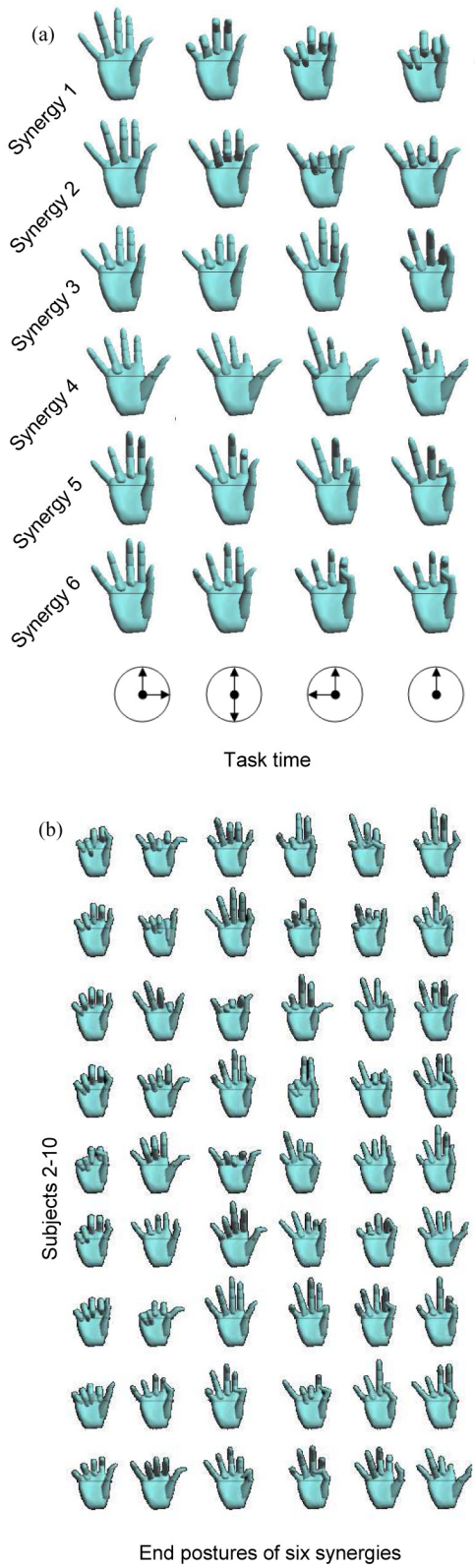

Fig. 6. (a) Postural synergies of subject 1. Each row corresponds to the temporal profile of one synergy. Each posture is a snapshot taken at discrete time steps (as indicated at the bottom of the figure) of the task. Synergies are arranged in the order of their significance with the first row (first synergy) being the most significant to the last row (last synergy) being the least significant. (b) Postural synergies of subjects 2–10. Each row corresponds to the end postures of six different synergies for one subject in the decreasing order of their significance from left to right.

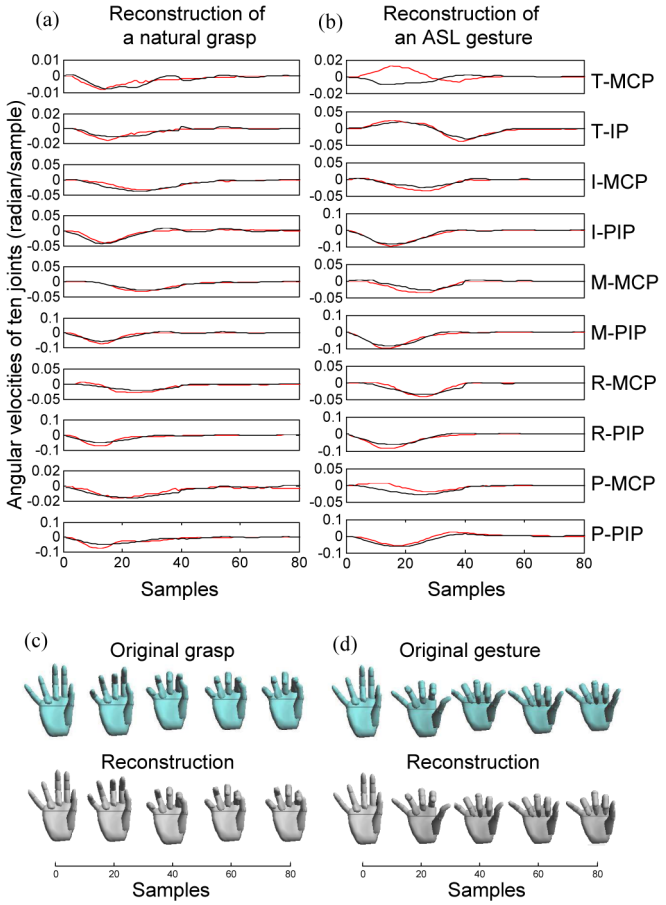

Fig. 7. Joint-angular-velocity profiles (in black) of a (a) natural grasping task and an (b) ASL gesturing task are reconstructed (in red) by using six synergies for subject 1. Postural snapshots are taken at discrete time steps for the previous natural grasp and reconstruction (c) and for the ASL gesture and reconstruction (d). See Fig. 5 for abbreviations of finger joints.

reconstructed. Examples of good reconstructions for natural grasping and ASL gesturing tasks are shown in the Fig. 7. As is clearly evident, the reconstructions were reasonably accurate using six synergies.

The reconstruction errors were calculated for each subject and each task for various numbers of synergies (PCs) by

$$\frac{\sum_{i=1}^{n}\sum_{t=1}^{T}\left[v_i^g(t)-\hat{v}_i^g(t)\right]^2}{\sum_{i=1}^{n}\sum_{t=1}^{T}v_i^g(t)^2}$$

where $\hat{v}_i^g(t)$ $(t=1,\ldots,T)$ is the angular-velocity profile of task g and finger joint i $(i=1,\ldots,n)$ reconstructed using a given number of synergies. Note that the previous reconstruction error is not a direct measure of the approximation error (quadratic difference between the original and reconstructed angular-velocity profiles) but expressed as a ratio between this approximation error and the size (also in quadratic sense) of the original angular-velocity profiles. The calculated reconstruction errors are shown in Fig. 8. The error bars indicate standard deviation across subjects averaged across 100 testing tasks for natural grasping and 36 tasks for ASL gesturing. The number of PCs versus reconstruction error plot also helps in determining the number of PCs. Although it is up to one's discretion about how many PCs can

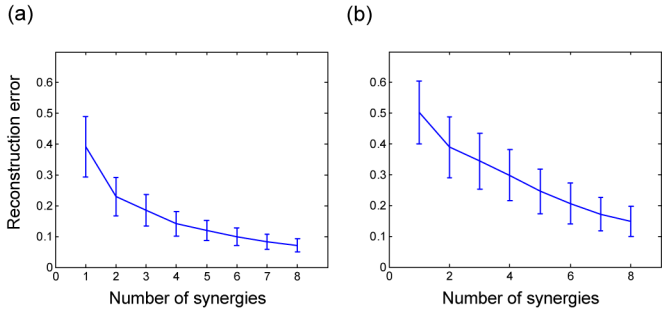

Fig. 8. Reconstruction error. The graphs illustrate the gradual decrease in the reconstruction error while recruiting synergies. Error bars indicate the standard deviation across subjects and tasks. (a) Reconstruction of natural grasps. (b) Reconstruction of ASL gestures.

be considered to account for appreciable reconstruction, in our case six synergies proved sufficient for reconstruction of the testing tasks. As a general observation, the reconstruction error of ASL tasks was greater than that of grasping tasks implying behavior specific nature of the synergies.

Fig. 9 shows the utilization of six synergies in reconstruction of a natural grasping task and an ASL gesturing task. These two tasks correspond to the tasks shown in Fig. 7(a) and (b), respectively. Heights of stems indicate the weights, and locations of stems indicate the shifts of particular synergy used in reconstruction. Synergies less than 10% of the maximum weight were not included. Discarding such synergies did not substantially alter the reconstruction errors. Miniplots in Fig. 9(a) and (b) show the shifted versions of synergies corresponding to locations of stems. The recruitment time indicates the amount of right shift of the synergy.

The previous results indicate that l_1-minimization was effective in the optimal selection of synergies minimizing the reconstruction error and, at the same time, using sparsest number of desirable synergies. In Fig. 9(a), sparsely selected shifted versions of synergies (11 selected out of a total of 264 shifted synergies) were used in reconstruction of the natural grasping task. This indicates that the synergies obtained during rapid tasks were able to reconstruct natural or slower movements. In contrast, in Fig. 9(b), the selected synergies, though still sparsely distributed (14 selected out of the 264 shifted synergies), were more than those used in the natural grasping task. Note that gesturing ASL postures is different in behavior when compared to grasping. Fig. 10(a) and (b) shows for subject 1 the numbers of synergy recruitments in reconstruction of 100 natural grasping tasks and 36 ASL gesturing tasks. Also in Fig. 10(c), a comparison is drawn between the numbers of recruitments of the six synergies (averaged across tasks—error bars indicating the standard deviation) in grasping tasks and ASL tasks for subject 1. It is observed that average recruitment of synergies is more for ASL tasks than for grasping tasks. Thus, the results indicate the behavior specific nature of the obtained synergies. This is corroborated in Fig. 11, where a comparison of synergy recruitments (averaged across tasks) between grasping tasks and ASL tasks is shown for subjects 2–10.

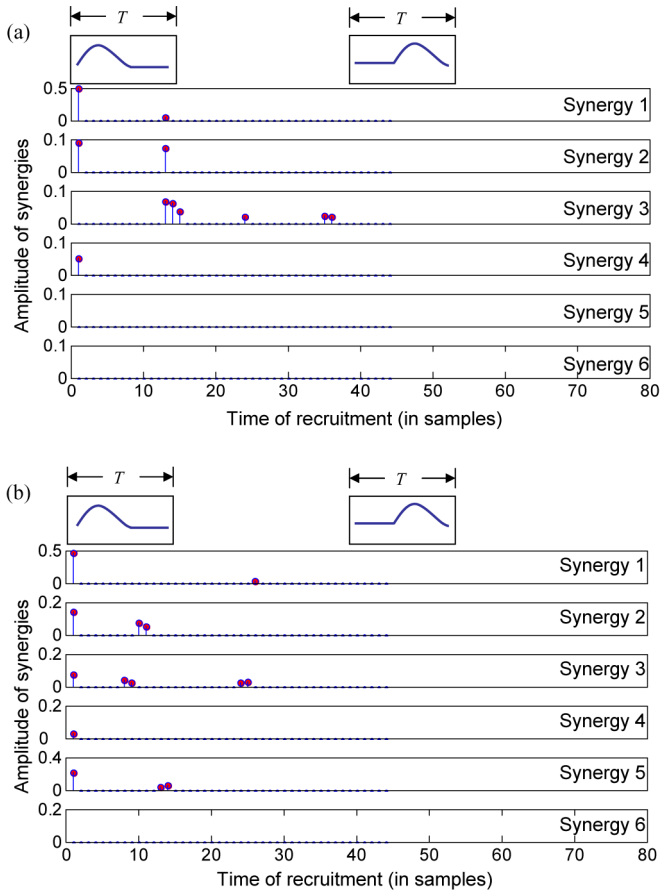

Fig. 9. Utilization of six synergies in reconstruction of a (a) natural grasping task [same as in Fig. 7(a)] and an (b) ASL gesturing task [same as in Fig. 7(b)]. Heights and locations of the stems indicate the weights and shifts, respectively, of particular synergies used in the reconstruction. Previous miniplots indicate the shifted versions of synergies corresponding to locations of stems. The recruitment time indicates the amount of right shift of the synergy. Sparseness of selection by l_1-minimization and multiple recruitments of synergies are evident in the plots.

IV. Discussion

A. Usage of Linear Convolutive-Mixture Model

In this paper, kinematic synergies were obtained based on a convolutive-mixture model for generation of hand movements. The model was then realized using l_1-minimization in recruitment of synergies. One might question the importance of these higher level models (including those input–output or black box models without touching details of internal system operations) as there have been a lot of advances in neuroanatomy and neurophysiology that can furnish the detailed functionality at neural and muscular levels. Growing importance of virtual reality and BCI, in the field of prosthetics and rehabilitation, is in need of similar higher level and computationally simpler models. For instance, single neuron recordings from monkey's motor cortex have been used in decoding arm movements [19]. In such experiments, where investigators record the central neural sources and the peripheral end postures of arms, the application of input–output models will play an important role. Although complex models have been proved helpful in offline analysis, they are

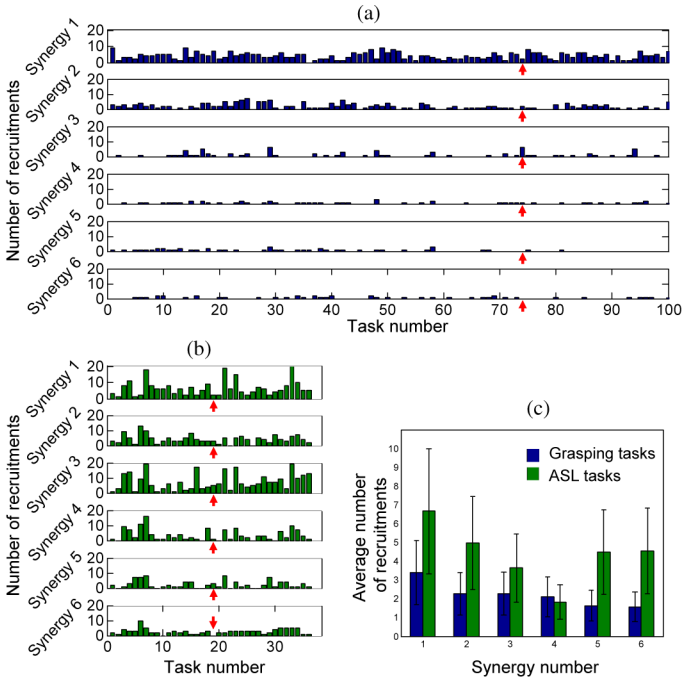

Fig. 10. Numbers of synergy recruitments in reconstruction of (a) 100 natural grasping tasks and (b) 36 ASL gesturing tasks for subject 1. Red arrows in (a) and (b) indicate the 74th grasping task [same as in Fig. 9(a)] and the 19th ASL task [same as in Fig. 9(b)], respectively. (c) Comparison of the numbers of recruitments of the six synergies (averaged across tasks—error bars indicating the standard deviation) in grasping tasks and ASL tasks.

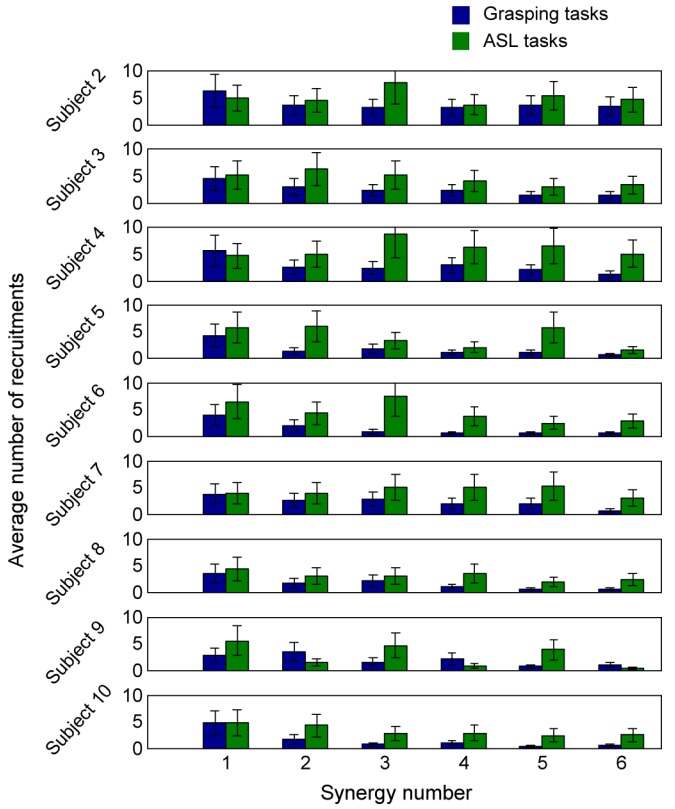

Fig. 11. Comparison of synergy recruitments (averaged across tasks) in grasping tasks and ASL tasks for subjects 2−10.

limited in online implementation as they demand lots of processing time. Computationally efficient models are necessary for BCI applications in real time.

The convolutive-mixture model offers more than curve fitting. The model expresses joint velocity profiles of hand as a weighted linear combination of time-varying movement modules or primitives. These movement modules when visualized have physiological significance [see the next section, and Fig. 6(a) and (b)]. Eigenpostures or postural synergies were reported to have physiological and anatomical significance by Mason *et al.* [4]. This implies that the model is not the same as rudimentary curve fitting with random movements.

The linear nature of the current model may be questioned as the neuromuscular system is nonlinear. However, considering a linear approximation might give useful insight of the system. Linear models have been employed by other studies. Humphrey used a linear systems model to relate neuronal firing rates to muscular torque [20]. Averbeck *et al.* [21] recorded neural activity from ensembles of neurons in areas of parietal cortex; in that study the linear model of hand kinematics outperformed the nonlinear model suggesting a reasonably linear relation between the neural activity and the hand velocity. A linear model by Moran and Schwartz [22] described a large portion of the time-varying velocity and direction in motor cortical activity. Moreover, the motor behavior of vertebrates has been approximated by linear combination of movement primitives [1], [23]. Following these studies, we consider using linear combination of synergies in solving how the CNS simplifies the problem of managing redundant DOFs of peripheral apparatus.

B. Velocity Profiles Versus Acceleration Profiles

Our model decomposed kinematic synergies in angular velocity profiles of joint angles. This study cannot answer whether neural signals encode velocity or acceleration—the question itself is debated in neurophysiology. Our model was motivated by the following studies. Moran and Schwartz [22] found that the time-varying speed of movement is represented in the cortical activity. Averbeck *et al.* [21] used linear models to successfully predict the hand velocity from the neural activities. Reports based on analyses of both single neurons and neural assemblies by Georgopoulos *et al.* [24] have provided evidence that neural populations in the primary motor cortex code movement direction and velocity. Thoroughman and Shadmehr [3] and Imamizu *et al.* [25] found that many Purkinje cells in the cerebellum simultaneously encode the direction and speed components of velocity. Also, during reaching movements firing rates of 80% of arm related mossy fibers correlated with joint angle, 33% correlated with velocity, and only a few were related to acceleration [26]. However, our model is not limited to velocity profiles. Position profiles were used in a similar model by us in [8]. The model can also be extended to acceleration profiles.

C. Time Scaling of Synergies

In this study time-shifted versions of synergies derived from rapid movements were used in reconstructing natural (slower) movements and ASL gestures. Intuitively, reconstructions will

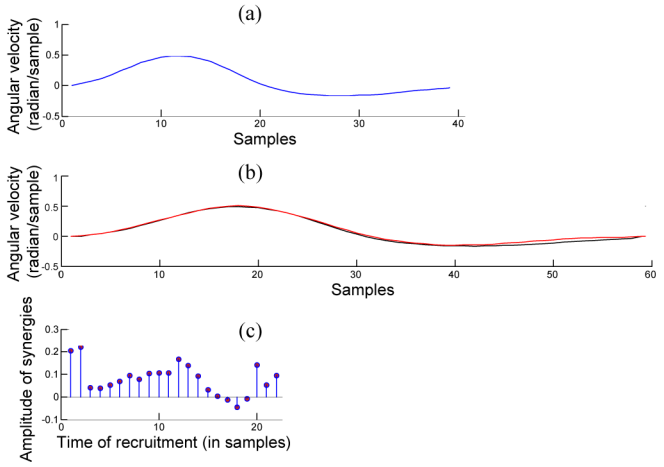

Fig. 12. Reconstruction of a dilated velocity profile. (a) Original velocity profile, which is used as template function in the reconstruction. (b) Dilated version of (a) (in black) is reconstructed (in red) from (a). (c) Utilization of (a) in reconstruction, where heights and locations of the stems indicate the weights and shifts, respectively, of the template function.

cost less number of synergies if time scaling, or in other words, dilation of synergies is allowed. A test case is illustrated in Fig. 12. A rapid joint velocity profile in Fig. 12(a) was used to reconstruct a dilated version of it, as shown in Fig.12(b). Recruitments of rapid joint velocity profile are shown in Fig. 12(c). From Fig. 12(c), it is observed that adjacent recruitments occur when the profile to be reconstructed is dilated. In Fig. 9(a) and (b), recruitments of synergies in reconstruction of the natural grasping and ASL gesturing tasks for subject 1 are shown. Adjacent recruitments can be seen for the third synergy in the grasping task and for the second, third, and fifth synergies in the ASL task. There exists neurophysiological evidence that the putamen of the basal ganglia in particular deals with scaling the movements [27]. Learned movement patterns are preserved at different speeds which is made possible by scaling of movement patterns. Introducing dilation for synergies might reduce the number of synergies recruited in reconstructions. But this would increase the burden on selection of synergies as the bank of synergies should not only accommodate shifted versions of synergies but also include dilated versions of synergies and their shifted versions. Although introducing dilation might improve reconstruction error and utilization of synergies, it might hinder the performance of the algorithm in real time. Performance tradeoffs in such conditions are to be analyzed. We view these as a future scope.

D. Insights Obtained From Temporal Postural Synergies

The temporal postural synergies were calculated by integrating the kinematic synergies. In Fig. 6(a), for the third, fifth, and sixth synergies in this subject, index finger acts as a master in leading the movement and rest of the fingers follow it as slaves. This concept has been observed previously and called enslaving [28]. Implementing such observations of biomechanical constraints in prosthetic hands can greatly reduce the complexity involved in computations. From the end postures in Fig. 6(a) and (b), it is clearly evident that the synergies are all unique. As a general trend across subjects, the synergies corresponded to flexion, extension, and pinch. This was supported in the recruitments of synergies in Fig. 10(a). The first grasping task, which is a full hand grasp of a sphere recruited first synergy more often than others. Flexion and extension synergies were recruited simultaneously to achieve intermediate closures of aperture. Also, the 74th grasping task [see Fig. 7(a)] recruited the pinch (the third) synergy as seen in Fig. 10(a) and is graphically verified as a pinch grasp in Fig. 7(c). In all of these synergies, it is clearly observed, as the size of the grasping object decreases the flexion at metacarpal joints increases. In the first synergy for subject 1, the metacarpal flexion was dominant when compared to other synergies and got lesser and lesser as we moved down. Also, for major movements only MCP joints were involved. For finer and precise movements after major movements, proximal and distal joints were recruited, respectively. This can be witnessed in the third synergy for subject 1, suggesting hierarchical recruitment of joints.

E. Multiple Recruitments of Synergies

In this paper, we have introduced the concept of multiple recruitments of synergies. There have been similar models of combination of movement primitives but none accommodated the possibility of multiple recruitments of synergies. Latash *et al.* [29] hypothesized that there are two types of libraries under which synergies are grouped—one library for day-to-day actions and the other library for learning novel actions—and that these synergies are borrowed as necessitated by environmental conditions. The current model facilitates the previous hypothesis. Here, the same synergy can be borrowed from one of the libraries more than once at different times with different amplitudes for execution of movement. A typical movement was expressed as a linear combination of a primary movement and delayed submovement in [30]. It was observed that the characteristics of shape and symmetry of the primary movement were similar to submovement. This implies that the same mechanism can be accomplished by a single synergy used multiple times avoiding use of two different primitives (one for primary and other for submovement).

F. Role of Synergies in Rehabilitation, Robotics, and BCI

This paper presents synergies not only as a hypothetical concept but with potential practical applications. Biologically inspired synergies are being used in stroke rehabilitation and in regaining lost motor functions in movement disorders. The concept of muscle synergies has been extended to examine the electromyogram (EMG) patterns in patients with stroke [31]. This study examines whether the motor disturbances following a stroke are the result of: 1) missing one or more synergies; 2) a failure of supraspinal structures to provide the correct coefficient of activation to one or more synergies; 3) a failure to select the proper synergies to accomplish a specific goal; or 4) a change in the balance of individual muscles within a given synergy. Bimanual coordination is damaged in brain lesions and neurological disorders. Study of the eigenpostures in normal subjects

during bimanual coordination and comparing them with bimanual eigenpostures of patients might have a potential contribution for rehabilitation [13]. By training, if such lacking eigenpostures are learned by patients, it might be possible to bring back the missing bimanual coordination. It is expected that synergies will provide immense help in future rehabilitation and diagnosis of movement disorders [8].

Added to growing neurophysiological attention, synergies are viewed to be crucial design elements in robotics. Based on the principle that vertebrates recruit kinematic synergies managing several joints, a control strategy for the balance of humanoid robots has been developed by Hauser *et al.* [32]. This control strategy reduces computational complexity while operating in real time following a biological framework that the CNS uses to handle numerous degrees of freedom. Biologically inspired synergies have also been considered in the study of artificial hands [33]. Moreover, synergies that facilitate data reduction and dimensionality reduction will soon find place in telesurgery and telerobotics [9].

BCI has been a promising technology for neural prosthesis. Despite the progress, however, BCI is still limited by the available number of independent control signals that can be extracted from human or primate brain. These pose limitations for brain control of multidimensional prosthesis like robotic hands and arms. Our study on synergies can be extended to address the earlier limitation. For example, assuming that only three independent control signals are available to us, we can use these three signals to command control in the low-dimensional space of synergies rather than in the high-dimensional space of joint movements (whose DOF can be more than 10 for a robotic hand). As shown in this paper, a small set of synergies suffices to reproduce a wide range of hand movements with sufficient flexibility. The authors are currently working on real-time control of virtual hand using synergies.

V. Conclusion

Based on a linear convolutive-mixture model for hand movement generation, this paper developed a method for decomposing joint-angular-velocity profiles of hand movements into kinematic synergies. The method split the decomposition process into two stages: 1) extracting the waveforms of synergies from rapid movement tasks using SVD, and 2) finding the weights and onset times of synergies based on l_1-minimization. The kinematic synergies were hypothesized to serve as building blocks in movement generation and provide solutions to the dimensionality reduction in control and coordination of the hand. The modular organization of synergies may be due to interactions between the higher level neural system (e.g., motor cortex), lower level neural system (e.g., spinal cord), and biomechanical structure. However, the complex interactions between these systems remain mysterious in the field of neurophysiology even today. The model proposed here is not limited to kinematic or postural synergies of any limb. It can be readily extended to muscular synergies. It can also be extended to include dynamics such as joint torques and forces to be useful in the design of actuator for robotic or prosthetic hands. We view these as our future scope.

Acknowledgment

The authors would like to thank the reviewers and editors for their valuable suggestions and comments.

References

[1] F. A. Mussa-Ivaldi, S. F. Giszter, and E. Bizzi, "Linear combination of primitives in vertebrate motor control," *Proc. Nat. Acad. Sci. USA*, vol. 91, no. 16, pp. 7534–7538, Aug. 1994.

[2] M. Santello, M. Flanders, and J. F. Soechting, "Postural hand synergies for tool use," *J. Neurosci.*, vol. 18, no. 23, pp. 10 105–10 115, Dec. 1998.

[3] K. A. Thoroughman and R. Shadmehr, "Learning of action through adaptive combination of motor primitives," *Nature*, vol. 407, no. 6805, pp. 742–747, Oct. 2000.

[4] C. R. Mason, J. E. Gomez, and T. J. Ebner, "Hand synergies during reach-to-grasp," *J. Neurophysiol.*, vol. 86, no. 6, pp. 2896–2910, Dec. 2001.

[5] A. d'Avella, P. Saltiel, and E. Bizzi, "Combinations of muscle synergies in the construction of a natural motor behavior," *Nature Neurosci.*, vol. 6, no. 3, pp. 300–308, Mar. 2003.

[6] T. E. Jerde, J. F. Soechting, and M. Flanders, "Coarticulation in fluent fingerspelling," *J. Neurosci.*, vol. 23, no. 6, pp. 2383–2393, Mar. 2003.

[7] M. C. Tresch, V. C. K. Cheung, and A. d'Avella, "Matrix factorization algorithms for the identification of muscle synergies: Evaluation on simulated and experimental data sets," *J. Neurophysiol.*, vol. 95, no. 4, pp. 2199–2212, Apr. 2006.

[8] R. Vinjamuri, D. Crammond, D. Kondziolka, H.-N. Lee, and Z.-H. Mao, "Extraction of sources of tremor in hand movements of patients with movement disorders," *IEEE Trans. Inf. Technol. Biomed.*, vol. 13, no. 1, pp. 49–56, Jan. 2009.

[9] R. Vinjamuri, Z.-H. Mao, R. Sclabassi, and M. Sun, "Time-varying synergies in velocity profiles of finger joints of the hand during reach and grasp," in *Proc. 29th Annu. Int. Conf. IEEE EMBS*, Lyon, France, Aug. 2007, pp. 4846–4849.

[10] M. C. Tresch, P. Saltiel, and E. Bizzi, "The construction of movement by the spinal cord," *Nature Neurosci.*, vol. 2, no. 2, pp. 162–167, Feb. 1999.

[11] Virtual Realities, Inc. (2009, Jul.). [Online]. Available: http://www.vrealities.com/cyber.html

[12] B. Yi, F. C. Harris, L. Wang, and Y. Yan, "Real-time natural hand gestures," *Comput. Sci. Eng.*, vol. 7, no. 2, pp. 92–96, May/Jun. 2005.

[13] R. Vinjamuri, M. Sun, D. Crammond, R. Sclabassi, and Z.-H. Mao, "Inherent bimanual postural synergies in hands," in *Proc. 30th Annu. Int. Conf. IEEE EMBS*, Vancouver, BC, Canada, Aug. 2008, pp. 5093–5096.

[14] *One handed sign language* [Online]. Available: http://www.signlanguagereviews.com/TypesOfSignLanguage/OneHandedSignLanguage.php.

[15] I. T. Jolliffe, *Principal Component Analysis*. 2nd ed. New York: Springer-Verlag, 2002.

[16] D. L. Donoho and M. Elad, "Optimally sparse representation in general (nonorthogonal) dictionaries via l^1 minimization," *Proc. Nat. Acad. Sci. USA*, vol. 100, no. 5, pp. 2197–2202, Mar. 2003.

[17] S. S. Chen, D. L. Donoho, and M. A. Saunders, "Atomic decomposition by basis pursuit," *SIAM J. Sci. Comput.*, vol. 20, no. 1, pp. 33–61, Aug. 1998.

[18] S.-J. Kim, K. Koh, M. Lustig, S. Boyd, and D. Gorinevsky, "An interior-point method for large-scale l_1-regularized least squares," *IEEE J. Sel. Topics Signal Process.*, vol. 1, no. 4, pp. 606–617, Dec. 2007.

[19] M. Velliste1, S. Perel, M. C. Spalding, A. S. Whitford, and A. B. Schwartz, "Cortical control of a prosthetic arm for self-feeding," *Nature*, vol. 453, no. 19, pp. 1098–1101, Jun. 2008.

[20] D. R. Humphrey, "Relating motor cortex spike trains to measures of motor performance," *Brain Res.*, vol. 40, no. 1, pp. 7–18, May 1972.

[21] B. B. Averbeck, M. V. Chafee, D. A. Crowe, and A. P. Georgopoulos, "Neural activity in prefrontal cortex during copying geometrical shapes. I. Single cells encode shape, sequence, and metric parameters," *Exp. Brain Res.*, vol. 150, no. 2, pp. 127–141, May 2003.

[22] D. W. Moran and A. B. Schwartz, "Motor cortical representation of speed and direction during reaching," *J. Neurophysiol.*, vol. 82, no. 5, pp. 2676–2692, Nov. 1999.

[23] T. Flash and B. Hochner, "Motor primitives in vertebrates and invertebrates," *Curr. Opin. Neurobiol.*, vol. 15, no. 6, pp. 660–666, Dec. 2005.

[24] A. P. Georgopoulos, J. F. Kalaska, R. Caminiti, and J. T. Massey, "On the relations between the direction of two dimensional arm movements and cell discharge in primate motor cortex," *J. Neurosci.*, vol. 2, no. 11, pp. 1527–1537, Nov. 1982.
[25] H. Imamizu, S. Miyauchi, T. Tamada, Y. Sasaki, R. Takino, B. Putz, T. Yoshioka, and M. Kawato, "Human cerebellar activity reflecting an acquired internal model of a new tool," *Nature*, vol. 403, no. 6766, pp. 192–195, Jan. 2000.
[26] N. Schweighofer, M. A. Arbib, and M. Kawato, "Role of the cerebellum in reaching movements in humans. I. Distributed inverse dynamics control," *Eur. J. Neurosci.*, vol. 10, no. 1, pp. 86–94, Jan. 1998.
[27] V. B. Brooks, *Neural Basis of Motor Control*. Oxford, UK: Oxford Univ. Press, 1986.
[28] C. L. Mackenzie and T. Iberall, *The Grasping Hand (Advances in Psychology)*. Amsterdam, The Netherlands: North-Holland, 1994.
[29] S. L. Gorniak, V. M. Zatsiorsky, and M. L. Latash, "Hierarchies of synergies: An example of two-hand multi finger tasks," *Exp. Brain Res.*, vol. 179, no. 2, pp. 167–180, May 2007.
[30] K. E. Novak, L. E. Miller, and J. C. Houk, "The use of overlapping submovements in the control of rapid hand movements," *Exp. Brain Res.*, vol. 144, no. 3, pp. 351–364, Jun. 2002.
[31] E. Bizzi, "Motor primitives and rehabilitation," in *Proc. 6th Int. Workshop Virtual Rehabil.*, Venice, Italy,, Sep.2007, pp. 20–22.
[32] H. Hauser, G. Neumann, A. J. Ijspeert, and W. Maass, "Biologically inspired kinematic synergies provide a new paradigm for balance control of humanoid robots," in *Proc. IEEE-RAS 7th Int. Conf. Humanoid Robots*, Pittsburgh, PA, Nov./Dec. 2007, pp. 73–80.
[33] M. Popovic and D. Popovic, "Cloning biological synergies improves control of elbow neuroprostheses," *IEEE Eng. Med. Biol. Mag.*, vol. 20, no. 1, pp. 74–81, Jan./Feb. 2001.

Ramana Vinjamuri (S'02–M'08) received the B.S. degree in electrical and electronics engineering from Kakatiya University, Warangal, India, in 2002, the M.S. degree in electrical engineering (specialized in bioinstrumentation) from Villanova University, Villanova, PA, in 2004, and the Ph.D. degree in electrical engineering (specialized in dimensionality reduction techniques in hand movements, prosthesis, robotics, and virtual reality) from the University of Pittsburgh, Pittsburgh, PA, in 2008.

He is currently a Postdoctoral Fellow in the Department of Physical Medicine and Rehabilitation, University of Pittsburgh, where he is engaged in the field of neural prosthesis through brain–computer interface.

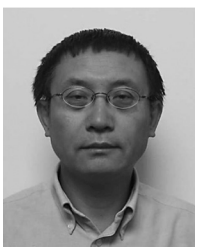

Mingui Sun (S'88–M'89–SM'05) received the B.S. degree from Shenyang Chemical Engineering Institute, Shenyang, China, in 1982, and the M.S. and Ph.D. degrees in electrical engineering from the University of Pittsburgh, Pittsburgh, PA, in 1986 and 1989, respectively.

In 1991, he joined the University of Pittsburgh, where he is currently a Professor of neurosurgery, electrical and computer engineering, and bioengineering. He is also the Director of Research at Computational Diagnostics, Inc., Pittsburgh. His current research interests include advanced biomedical electronic devices, biomedical signal and image processing, sensors and transducers, biomedical instruments, artificial neural networks, wavelet transforms, time–frequency analysis, and the inverse problem of neurophysiological signals. He has authored or coauthored more than 200 publications.

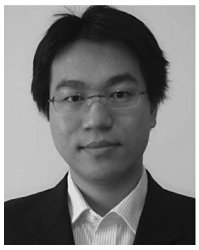

Cheng-Chun Chang (S'06–M'09) received the B.Sc. degree from National Tsing Hua University, Hsinchu, Taiwan, in 2001, the M.Sc. degree from National Taiwan University, Taipei, Taiwan, in 2003, and the Ph.D. degree from the University of Pittsburgh, Pittsburgh, PA, in 2008, all in electrical engineering.

He was with the Johns Hopkins University in 2005 for Post-Master's study. He joined the start-up company, Nanolambda, in 2009, where he was a Principal Engineer and was in charge of algorithm development for applications of nano-optical-filter-array spectrum sensors. Since August 2009, he has been an Assistant Professor in the Department of Electrical Engineering, National Taipei University of Technology, Taipei. His current research interests include the general area of DSP, wireless communications, and the application of signal processing techniques to optical and biomedical applications.

Heung-No Lee (S'94–M'99) was born in Choong-Nam, Korea. He received the B.S., M.S., and Ph.D. degrees in electrical engineering from the University of California, Los Angeles (UCLA), in 1993, 1994, and 1999, respectively.

From 1999 to 2001, he was with the Network Analysis and Systems Department, Information Science Laboratory, Hughes Research Laboratories, Malibu, CA, where he led a number of research projects as Principal Investigator (PI). In 2002, he joined as an Assistant Professor the Department of Electrical Engineering, University of Pittsburgh, Pittsburgh, PA, where he started the Communications Research Laboratory in 2002. At the University of Pittsburgh, he led a number of research projects as PI or co-PI supported by the National Science Foundation (NSF), Pittsburgh Digital Greenhouse (the Technology Collaborative), Adcus, and NanoLambda. Since 2009, he has been an Associate Professor with the Department of Information and Communications, Gwangju Institute of Science and Technology, Gwangju, Korea. His current research interests include information, channel coding, communications, and signal processing theories for wireless networking and biomedical applications.

Robert J. Sclabassi (M'62–S'68–SM'93) received the B.S.E. degree in electrical engineering from Loyola University, Los Angeles, CA, the M.S.E.E. and Ph.D. degrees in electrical engineering from the University of Southern California, Los Angeles, and the M.D. degree in medicine from the University of Pittsburgh, Pittsburgh, PA.

He was with the Advanced Systems Laboratory at TRW, Los Angeles, and a Postdoctoral Fellow at the Brain Research Institute, University of California, Los Angeles (UCLA), where he has also been a Faculty Member in the Department of Neurology and Biomathematics. He is currently a Professor of neurological surgery, psychiatry, electrical engineering, mechanical engineering, and behavioral neuroscience at the University of Pittsburgh. He has authored or coauthored more than 400 papers, chapters, and conference proceedings.

Prof. Sclabassi is a Registered Professional Engineer.

Zhi-Hong Mao (S'96–M'05–SM'09) received the dual B.S. degrees in automatic control and applied mathematics and the M.Eng. degree in intelligent control and pattern recognition from Tsinghua University, Beijing, China, in 1995 and 1998, respectively, the S.M. degree in aeronautics and astronautics from Massachusetts Institute of Technology (MIT), Cambridge, in 2000, and the Ph.D. degree in electrical and medical engineering from the Harvard–MIT Division of Health Sciences and Technology, Cambridge, in 2005.

Since 2005, he has been an Assistant Professor in the Department of Electrical and Computer Engineering and the Department of Bioengineering, University of Pittsburgh, Pittsburgh, PA.